

Pruning vs XNOR-Net: A Comprehensive Study of Deep Learning for Audio Classification on Edge-devices

MD MOHAIMENUZZAMAN¹, CHRISTOPH BERGMEIR¹ AND BERND MEYER¹

¹Department of Data Science and AI, Monash University, Australia (e-mail: md.mohaimen, christoph.bergmeir, bernd.meyer@monash.edu)

Corresponding author: Md Mohaimenuzzaman (e-mail: md.mohaimen@monash.edu).

ABSTRACT Deep Learning has celebrated resounding successes in many application areas of relevance to the Internet-of-Things, for example, computer vision and machine listening. To fully harness the power of deep learning for the IoT, these technologies must ultimately be brought directly to the edge. The obvious challenge is that deep learning techniques can only be implemented on strictly resource-constrained edge devices if the models are radically downsized. This task relies on different model compression techniques, such as network pruning, quantization, and the recent advancement of XNOR-Net. This paper examines the suitability of these techniques for audio classification on microcontrollers. We present an XNOR-Net for end-to-end raw audio classification and a comprehensive empirical study comparing this approach with pruning-and-quantization methods. We show that raw audio classification with XNOR yields comparable performance to regular full precision networks for small numbers of classes while reducing memory requirements 32-fold and computation requirements 58-fold. However, as the number of classes increases significantly, performance degrades, and pruning-and-quantization based compression techniques take over as the preferred technique being able to satisfy the same space constraints but requiring about 8x more computation. We show that these insights are consistent between raw audio classification and image classification using standard benchmark sets. To the best of our knowledge, this is the first study applying XNOR to end-to-end audio classification and evaluating it in the context of alternative techniques. All code is publicly available on GitHub.

INDEX TERMS Sound Classification, Audio Classification, Deep Learning, Model Compression, Filter Pruning, Channel Pruning, XNOR-Net, Edge-AI, Microcontroller, and Image Classification

I. INTRODUCTION

AUDIO classification is a fundamental building block of many smart IoT applications such as predictive maintenance [1]–[3], surveillance [4], and ecosystem monitoring [5], [6]. Smart sensors driven by microcontroller units (MCUs) are at the core of these applications. MCUs, installed at the edge of the networks, sense data and send them to the cloud for classification and detection. However, the energy requirement for transmitting the high volumes of data becomes a burden for the battery powered MCUs. Furthermore, this increases latency and data transmission may further lead to privacy concern. The increased latency makes real-time or near real-time analytics infeasible. One way to solve these challenges is to move the analysis and recognition directly to the edge. In practice this means that all processing must take place on resource impoverished MCUs.

MCUs are low-powered resource-constrained devices typically based on system-on-a-chip (SoC) hardware with less than a megabyte (1 MB) of RAM and below 200 MHz clock speeds. All the recent state-of-the-art audio classification models, however, are based on Deep Learning (DL) [7]–[15] requiring very resource-intensive computation. Usually, the memory size of such models varies from several MBs to even gigabytes (GB). To run such models on MCUs requires extreme minimization of the model's size and computation requirements with minimum loss of accuracy. Recent studies have applied model compression techniques such as pruning connections and neurons from Fully Connected Neural Networks (FCNN) [16], filter or channel pruning from Convolutional Neural Networks (CNN) [17]–[19], Knowledge Distillation [20] and low precision quantization [16], [21]. The most recent advancement for extreme downsizing of

DL models and their computation requirements is XNOR-Net [22] where a model's activations and inputs are fully binarized.

There are many state-of-the-art XNOR-Net models for different computer vision tasks, such as Rastegari *et al.* [22] for MNIST, Cong [23] for CIFAR-10, and Bulat *et al.* [24] for CIFAR-100 and Imagenet datasets. However, for audio classification, the only work we are aware of is presented by Cerutti *et al.* [25]. This work uses XNOR-Net in combination with spectrogram-based input, effectively performing audio classification via image classification. As the literature on full-precision audio networks shows, this approach does not usually deliver the best results for difficult classification problems with conventional CNN architectures [26], [27] (see Section II-B for further details). To the best of our knowledge, the current literature has not yet considered XNOR-Net for raw audio classification.

Most of the work on XNOR has been performed for computer vision. The leaderboards of benchmark image datasets show considerable difference in classification accuracy of state-of-the-art full precision nets and XNOR-Nets (see Table 8 for CIFAR-100 and Imagenet datasets). Furthermore, models produced by XNOR-Net generally require up to $32\times$ less memory and $58\times$ less computation than their full-precision counterparts [22], which may not guarantee sufficient reduction for MCUs. The memory requirements of XNOR-Net based DL models producing comparable accuracy [22]–[24] typically reach several MBs, while typical MCUs offer only 128KB to 1MB memory.

In this paper, we seek to understand the comparison of XNOR model minimization with pruning-and-quantization approaches and the potential of XNOR in the context of audio classification. We present XNOR-Nets for raw audio classification followed by a comprehensive study that compares this approach with traditional model compression techniques (pruning-and-quantization). Our extensive experimental study reveals that XNOR-Net may be preferred for scenarios comprising a small number of classes (e.g., 10 classes) along with extremely tight resources constraints, specifically where computation speed is concerned. In contrast, for complex scenarios with a larger number of classes, pruning-and-quantization based compression techniques would still be the choice as they produce sufficiently small models for off-the-shelf MCUs that have higher performance in terms of accuracy.

Experiments show that, when two models are generated by pruning-and-quantization and XNOR-Net for the same memory constraint, XNOR-Net requires $\sim 8\times$ less computation while both produce comparable classification accuracy for small problem sizes (number of classes). While XNOR-Nets require extremely little computation compared to their pruning-and-quantization based counterparts, their classification performance on datasets degrades rapidly with an increasing number of classes. The performance loss of pruning-and-quantization based models for the same audio benchmarks is much more graceful, so that this approach

still appears to be preferable for problems with larger class numbers.

To harden the above findings, we have conducted a similar study on image classification datasets and analyzed this in the context of current state-of-the-art full precision and XNOR-Net leaderboards for various image benchmarks. The behavior is found to be consistent in both the audio and the image domain.

Thus, the contribution of this paper is two-fold: 1) it presents the first XNOR-Net for raw audio classification as a benchmark for future research. 2) it presents the first comprehensive empirical comparison of pruning, quantization and XNOR-Net based model compression techniques and derives guidelines for when to use pruning, quantization, and binary networks, respectively.

II. BACKGROUND AND RELATED WORK

A. AUDIO REPRESENTATIONS

Audio can be represented in the time-domain as a wave form of amplitude changes over time (Figure 1). If this time series is directly used as input to the network, we speak of raw audio classification.

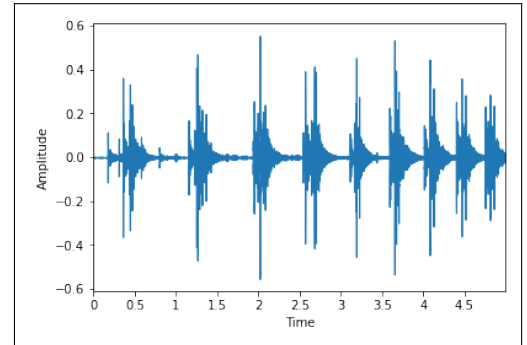


FIGURE 1. 1-D representation of audio as wave

An alternative is to use spectrograms. For this, the audio is first transformed into the frequency domain using Fourier transforms of short overlapping windows and presented with respect to time, frequency, and amplitude (Figure 2). The spectrogram captures the intensity of different frequency component of the signal against time (see Figure 3).

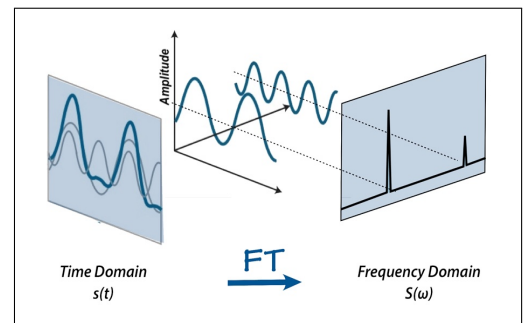


FIGURE 2. 2-D representation of audio [28].

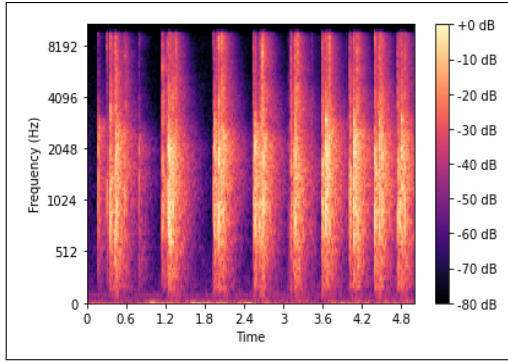


FIGURE 3. Example spectrogram

B. AUDIO FEATURE PROCESSING

The input representation is a fundamental decision when applying deep learning to any problem. Motivated by the tremendous success of deep learning in the image processing domain, researchers have used spectrograms directly as the input representation [27], [29]. Somewhat surprisingly, the results achieved so far have not matched the performance that might have been expected based on the state-of-the-art in visual image processing [26], [27].

While being a visual structure, spectrograms have different properties from natural images. A pixel of a certain color or the similar neighboring pixels of an image may often belong to the same visual object. On the other hand, although frequencies move together according to a common relationship of the sound, a particular frequency or several frequencies does not belong to a single sound [26], [27]. Furthermore, in images both axes carry spatial information, but the axes of spectrograms have different meanings. Sounds are not static two-dimensional objects like images, they genuinely are time series. The invariances in natural images and in spectrograms are thus fundamentally different. For example, moving a face in any direction does not change the fact that it is the same face. However, moving frequencies upwards may not only change an adult voice to a child voice or something completely different, it may also change the spatial information of the sound [27].

Hence, this research considers audio classification using raw audio time series, an approach that has proven to be successful with traditional full precision networks [9].

C. AUDIO CLASSIFICATION AT THE EDGE

The recent state-of-the-art performances for audio classification are all produced by different resource intensive DL models [9], [12]–[15]. These models need to be extremely compressed to be run on MCUs.

1) Model Compression

There are different DL model compression techniques such as un-structured model compression or weight pruning [16], structured compression or channel/filter/neuron pruning [18], [19], knowledge distillation [20], quantization [21] etc. Un-structured pruning produces sparse weight matrices and re-

quires sparse computation to fully utilize its benefits. This is not yet supported by MCUs [30]–[34]. Knowledge distillation is a very different approach to pruning where the knowledge of a large teacher network is transferred into a smaller student network. However, [9] shows that structured pruning produces superior performance to knowledge distillation in audio classification tasks. Hence, this study focuses on structured pruning and quantization as the alternative for compressing DNN models. For simplicity, we refer to this as “pruning-and-quantization.”

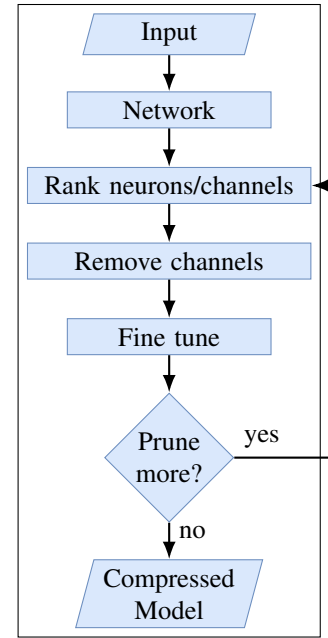


FIGURE 4. Iterative process of structured model compression

Structured pruning is an iterative process where a single iteration performs a global ranking of filters/neurons, followed by the removal of the lowest-ranked neuron/filter from the network and retraining of the network for one or two epochs to recover the loss of accuracy due to the pruning [18]. The ranking of filters/neurons is done using various ranking algorithms based on L2-Norm, Taylor criteria [18] and binary index-based ranking [35]. This is repeated until the target number of filters/neurons are removed from the network to find a model of desired size (see Figure 4).

Much work has been done on structured compression work for computer vision (e.g. [18], [19], [30], [31], [33], [34]). However, in the audio domain [9] is the only work so far that takes a state-of-the-art CNN model for audio classification, compresses it using a hybrid structured pruning technique, and quantizes the model using 8-bit post training quantization technique until a model is obtained that is fully deployed on an MCU. This work incorporates Taylor expansion criteria (TE) [18] in the ranking process. At first, a forward pass with the whole training dataset takes place and the gradient is applied to the activations to determine the least affected channels for ranking. The change in gradient can be presented as:

$$\Theta_{TE}(Z_l^i) = |\Delta C Z_l^i| \quad (1)$$

where Z_l^i is the i th feature map of layer l , ΔC is the change in loss denoted by $\frac{\delta C}{\delta Z_l^i}$ and $\Theta_{TE}(Z_l^i)$ denotes the change determined by TE. Now the gradient is applied to the activation as:

$$Z_l^i = Z_l^i + \Theta_{TE}(Z_l^i) \quad (2)$$

For the ranking of the channels, all the feature maps are normalized layer wise. Thus, the normalization for a layer l of a network can be expressed as:

$$\bar{Z}_l = \frac{|Z_l^{(i)}|}{\sqrt{\sum |Z_l|^2}} \quad (3)$$

where Z_l is the list of activations for all the channels c of a layer l in a CNN. Now, the ranking of the channels across all layers is performed and the index of the lowest ranked channel is determined as:

$$i_{lc} = \kappa(\bar{Z}) \quad (4)$$

where \bar{Z} are the normalized activations of all channels of all layers, κ is the function that takes \bar{Z} and returns the information of the channel having lowest magnitude i_{lc} where i is the index of channel c of layer l .

Once this iterative process produces the final compressed and fine-tuned model, it is further compressed using low precision quantization. Quantization is an independent process, and this study uses 8-bit quantization to achieve a further $4\times$ compression.

2) XNOR-Net

In a XNOR-Net [22], all the layers except the first and the last layer are binary. The input, activations and the weights of the binary layers are represented using either +1 or -1 and are stored efficiently with single bits. Figure 5 shows the construction of a typical convolution layer and the equivalent binary convolution layer.

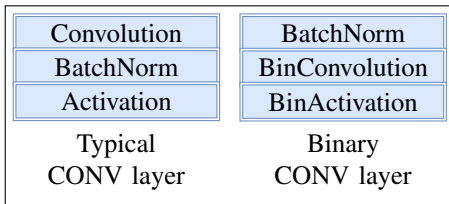


FIGURE 5. Typical convolution layer vs binary convolution layer

The convolutions between the matrices (input/activations and weights) are implemented using XNOR and bit-counting operations. For this, the convolution between two vectors $\in \mathbb{R}^n$ is approximated by the dot products between two vectors $\in \{-1, +1\}^n$ [22]. Thus, the convolution between input X and weight W can be written as:

$$Z \approx (\text{sign}(X) \odot \text{sign}(W)) \odot \alpha\beta \quad (5)$$

where α and β denotes the scaling factors for all the sub tensors in input X and weight W respectively and \odot denotes element-wise multiplication. Due to the binary activations the dot product between $\text{sign}(X)$ and $\text{sign}(W)$ can be replaced by XNOR and pop-count operations which require extremely little computation. Hence, Equation 5 reduces to:

$$Z \approx (X' \circledast W') \odot \alpha\beta \quad (6)$$

where $X' = \text{sign}(X)$, $W' = \text{sign}(W)$ with all zeros replaced by -1 and \circledast denotes the XNOR and pop-count operations between X' and W' . This process is extremely efficient in terms of memory and energy usage. According to Rastegari et al. XNOR-Net requires $32\times$ less memory and reduces $58\times$ computation requirements [22]. Figure 6 provides an example of how the dot product between $\text{sign}(X)$ and $\text{sign}(W)$ is replaced by XNOR and pop-count between X' and W' .

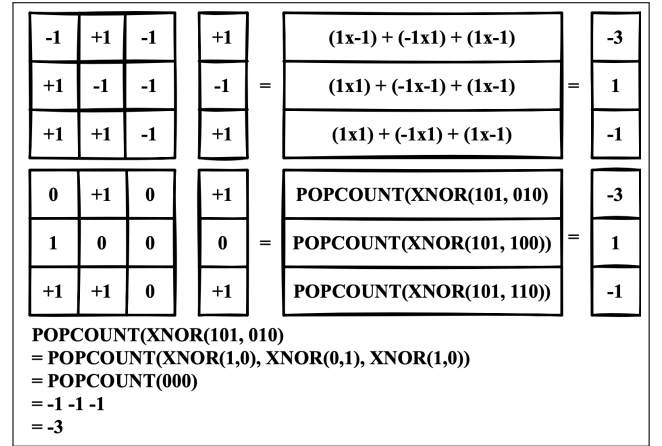


FIGURE 6. XNOR and POPCOUNT in XNOR-Net

There are state-of-the-art XNOR-Net models for different benchmark image datasets such as MNIST [22], CIFAR-10 [23], and CIFAR-100 and Imagenet datasets [24]. For audio data, we have found [25] to be the only work that has applied XNOR-Net.

III. ANALYSIS: PRUNING VS XNOR-NET

In this section, we compare pruning-and-quantization techniques with XNOR-Nets for raw audio classification. Our analysis through extensive experiments on different standard benchmark datasets for audio classification shows that XNOR is more effective for relatively simple problems and very tight constraints on the computational resources but that the higher classification accuracy achieved by pruning-and-quantization outweighs the benefit XNOR-Net for problems with complex data characteristics, large number of classes etc.

As our starting point for pruning-and-quantization techniques, we use one of the recent state-of-the-art DL networks for raw audio classification called ACDNet [9] and build derivatives of this using pruning-and-quantization as well as XNOR. We test these models on three standard benchmark

sound classification datasets - ESC-10 [36], ESC-50 [36], UrbanSound8k [37] and on subsets of these for an in-depth analysis on the effect of increasing numbers of classes. We create subsets of a dataset S_n with n classes as:

$$S_x \subseteq S_n \mid x \in \{10, 20, \dots, [n]\} \quad (7)$$

We measure classification accuracy through 5-fold cross validation. Full experimental details are provided in Section IV.

A. PRUNING-AND-QUANTIZATION

We have used the hybrid structured pruning technique proposed in [9] to derive Micro-ACDNet by pruning 80% of the channels from ACDNet. The trained model is first sparsified using l_0 norm. It can be expressed as:

$$\hat{Z} = W[\chi(W)] \quad (8)$$

where W are the weights of all the layers of the network and χ is the function that sorts W and returns the indices of the bottom 95% of the weights. The channels are then ranked, and the lowest ranked channel is removed from the network using Equations 1, 2, 3 and 4. The resulting model using this iterative pruning and fine-tuning process is called Micro-ACDNet [9]. Micro-ACDNet is quantized using a post-training 8-bit quantization technique. We refer to this quantized model as QMicro-ACDNet. The memory and computation requirements of QMicro-ACDNet make it suitable for current of-the-shelf MCUs (see Table 1). Micro-ACDNet and QMicro-ACDNet require $36x$ and $144x$ less memory, respectively, than ACDNet that requires 18.06MB to store its 4.74M parameters. Furthermore, both smaller versions require $37x$ less FLOPs compared to the base model. We note that QMicro-ACDNet requires the same number of FLOPs as Micro-ACDNet but only at quarter precision. If a full 32-bit FPU is used, this is not going to make a practical difference, but it allows us to exploit significant speed gains using 16-bit FPUs, 16-bit FPU modes on full precision FPUs, and software emulations when no hardware FPU is available.

Networks	Params (M)	Size (KB)	FLOPs (M)
ACDNet	4.74	18498	544
Micro-ACDNet	0.31	514	14.82
QMicro-ACDNet	0.31	128.5	14.82

TABLE 1. Size and computation requirements for ACDNet, Micro-ACDNet and QMicro-ACDNet

Although the smaller models require less resources, they lose classification accuracy as they have less capacity to learn. According to [9], Micro-ACDNet has 80% less capacity than ACDNet and QMicro-ACDNet is a quarter precision version (8-bit) of Micro-ACDNet. Table 2 and Figure 7 present the comparison of accuracy achieved by the three versions of the network on ESC-10, ..., 50 datasets (derived using Equation 7). For further details, see Section IV-A). The table and the figure show that all the three versions of the network produce state-of-the-art and near state-of-the-art accuracy on ESC-10, however, the accuracy drops

continuously with an increase in the number of classes, as may be expected.

#Classes	ACDNet	Micro-ACDNet	
	Full Precision	Full Precision	Quantized
10	96.75	96.25	92.75
20	92.38	90.13	82.55
30	89.25	86.83	81.67
40	85.94	81.56	75.71
50	87.05	83.25	75.50

TABLE 2. Accuracy (%) of ACDNet, Micro-ACDNet and QMicro-ACDNet on ESC-10, ..., 50 datasets

The base ACDNet achieves an accuracy of 96.75% and 87.05% on ESC-10 and ESC-50, respectively, whereas Micro-ACDNet produces 96.25% and 83.25% on ESC-10 and ESC-50, respectively. The quantized version experiences a larger drop in accuracy with the increase of the number of classes starting at 92.75% for ESC-10 and ending with 75.50% for ESC-50. Figure 7 shows the trends clearly.

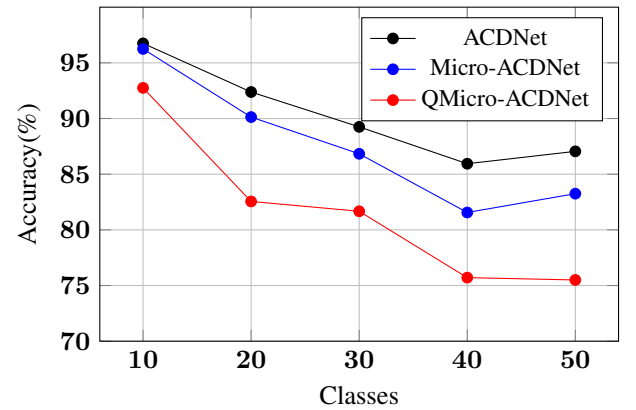


FIGURE 7. Accuracy (%) of ACDNet, Micro-ACDNet and QMicro-ACDNet on ESC-10, ..., 50 datasets

The scenario is no different when we apply the same networks on UrbanSound8k dataset. Table 3 shows that QMicro-ACDNet has loses almost 13.5%-points of accuracy compared to the base network. We note that specialized quantization targeted to a particular model can potentially reduce the loss of the accuracy that the models experience during the quantization process. However, improving any technique used to demonstrate the process is beyond the scope of this paper and while a change of quantization techniques may shift the results, the general trends would be expected to remain the same.

Networks	Accuracy (%)
ACDNet	84.45
Micro-ACDNet	78.28
QMicro-ACDNet	70.93

TABLE 3. ACDNet, Micro-ACDNet and QMicro-ACDNet accuracy on UrbanSound8k dataset

B. XNOR-NET

From Table 4 we see that the memory required by an XNOR-Net version of ACDNet (XACDNet) is 578KB. This is still too much for typical MCUs offering less than 1 MB of RAM, since this is just parameter space and already leaves hardly any room for the actual computations. Hence, we need a smaller version of the original network whose resource requirements do not exceed the resources available in MCUs. To compare the networks performance, memory, and computation requirements with QMicro-ACDNet, we create Mini-ACDNet such that its XNOR-Net version has similar requirements to QMicro-ACDNet (see Tables 1 and 4). To derive Mini-ACDNet, we use the same technique as the one to derive Micro-ACDNet, summarized above and fully detailed in [9].

Table 4 shows the memory and the computation requirements of the full precision networks and their XNOR counterparts. The sizes of the XNOR version of ACDNet (XACDNet) and Mini-ACDNet (XMini-ACDNet) are calculated according to [22]. The number of binary operations required for the networks are calculated according to [38]. We express the computation (Binary Operation + FLOPs) required for an XNOR network as FLOPs for simplicity. If a and b are the FLOPs required for the first and the last full precision layers of the XNOR network and x is the total amount of FLOPs of the full precision version of the network, then the calculation of FLOPs of an XNOR network can be expressed as $FLOPs = a + (x - (a + b))/64 + b$.

Networks	Params (M)	Size (KB)	FLOPs (M)
ACDNet	4.74	18498	544
XACDNet	4.74	578	8.88
Mini-ACDNet	1.05	4096	112
XMini-ACDNet	1.05	128.5	1.86

TABLE 4. Size and computation requirements for ACDNet, Mini-ACDNet and XMini-ACDNet

According to Table 4, XMini-ACDNet is extremely small (128.5KB) and requires considerably less computation. This clearly allows the network to be deployed on current off-the-shelf MCUs. Furthermore, from Table 5, we can see the XNOR networks produce reasonable accuracy for a smaller number of classes (ESC-10 with 10 classes). However, as the number of classes increases the network performance of the XNOR versions decreases rapidly.

Classes	ACDNet		Mini-ACDNet	
	Full Precision	XNOR	Full Precision	XNOR
10	96.75	91.25	96.75	82.25
20	92.38	77.25	91.12	54.75
30	89.25	70.42	88.58	46.83
40	85.94	61.87	84.50	38.56
50	87.05	56.40	85.60	31.70

TABLE 5. XNOR versions of ACDNet and Mini-ACDNet on ESC datasets

Figure 8 provides the performance graph of ACDNet, Mini-ACDNet along with their pruning-and-quantization and XNOR counterparts. The line at the bottom (XMini-ACDNet) shows how extremely the smallest XNOR-Net is affected when the number of classes increases, while QMicro-ACDNet manages to degrade much more gracefully. For both XNOR-Net networks (XACDNet and XMini-ACDNet), the slope is much steeper than for the other compression methods.

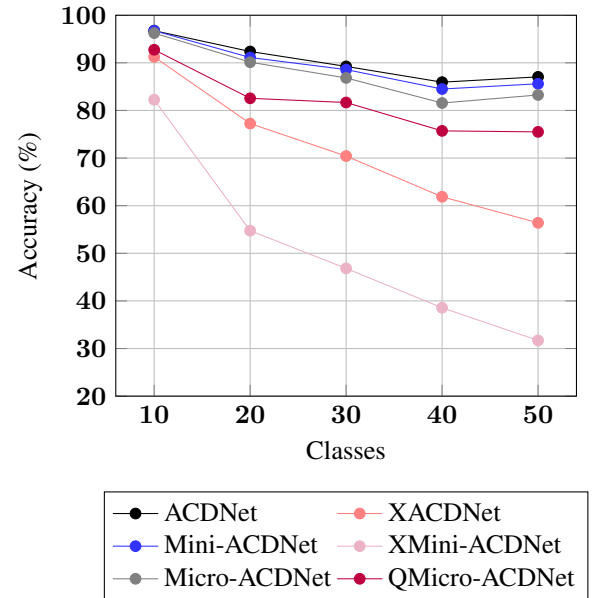


FIGURE 8. Comparison between Full Precision, Quantized and XNOR on ESC

Figure 9 provides the performance of the same networks on the UrbanSound8k dataset, another widely used audio benchmark. From the graph, we observe that the results for UrbanSound8k confirm our findings for ESC10...ESC50.

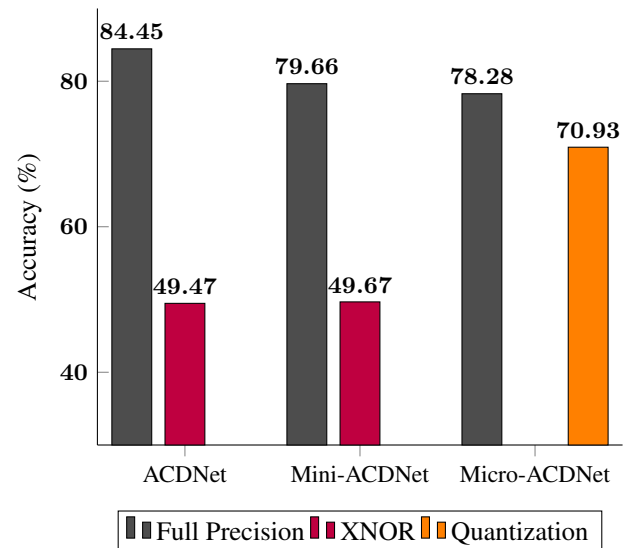


FIGURE 9. ACDNet, Micro-ACDNet and Mini-ACDNet accuracy on UrbanSound8k dataset.

In summary, we observe that the memory requirements of QMicro-ACDNet and XMini-ANDNet are essentially the same. XMini-ANDNet requires **7.97x** less FLOPs than QMicro-ACDNet. However, the XNOR-based models do not reach comparable classification accuracy when the number of classes is larger. Although the pruning-and-quantization based QMicro-ACDNet also sees a loss in accuracy, it still produces a reasonable classification accuracy for larger problems given its minuscule model size.

C. EXTENDED ANALYSIS

To the best of our knowledge, Cerutti *et al.* [25] have presented the only XNOR network for audio classification so far, termed BNN-GAP8. They have used a different benchmark, namely the less commonly used AudioEvent dataset [39]. We cannot test BNN-GAP8 on the most widely used benchmarks, ESC50 and Urbansound-8k, since BNN-GAP8 has not been described in sufficient detail in [25] to make it reproducible.

To facilitate a direct comparison, we extend our analysis to this dataset, which has also been used in a couple of other studies [39], [40]. The results are consistent with what we have seen above for the most widely used standard benchmarks. Table 6 and Figure 10 show the performance of our base nets on the AudioEvent dataset and its smaller subsets.

#Classes	ACDNet	Micro-ACDNet		Mini-ACDNet	
	Full Precision	Full Precision	Quantized	Full Precision	XNOR
10	96.25	95.66	94.08	95.86	74.16
20	92.82	90.03	86.71	92.93	53.48
28	92.57	89.69	84.98	92.49	43.4

TABLE 6. Accuracy (%) of ACDNet, Micro-ACDNet and QMicro-ACDNet on AudioEvent-10,20,28 datasets

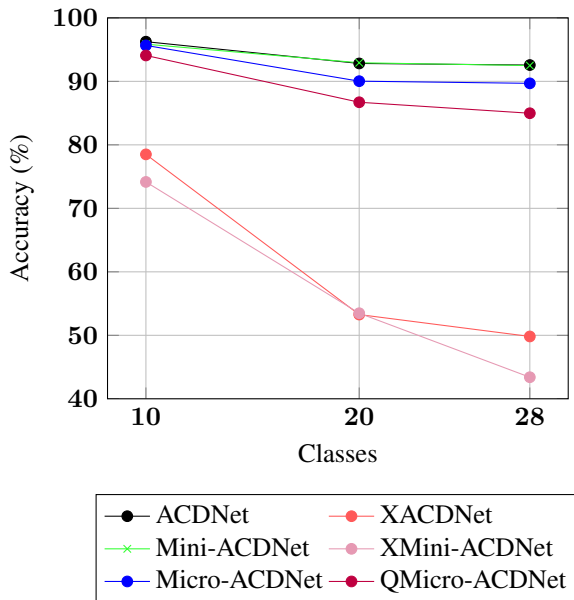


FIGURE 10. Comparison between Full Precision, Quantized and XNOR on AudioEvent datasets

However, larger resource requirements of our base networks do not allow us a direct and fair comparison to the

BNN-GAP8 network presented in [25]. We therefore derive two additional smaller networks with memory requirements equivalent to BNN-GAP8. QNano-ACDNet is an 8-bit quantized network derived by pruning and quantization (from the associated full-precision network Nano-ACDNet) and XACDNet-GAP8 is an XNOR network derived from the full precision network ACDNet-GAP8. The new models are constructed using the same procedures as described above. The tests of these networks on the AudioEvent dataset used in [25] are summarized in Table 7.

Networks	Accuracy	Memory (KB)	FLOPs (M)
CNN-CNP [40]	85.1	1766	2478
BNN-GAP8 [25]	77.9	58	1768
Nano-ACDNet	86.22	245	19
QNano-ACDNet	82.34	61	19
ACDNet-GAP8	90.35	1960	94
XACDNet-GAP8	35.48	61	2.2

TABLE 7. Accuracy (%) of BNN-GAP8, Nano-ACDNet and ACDNet-GAP8 on AudioEvent (has 28 classes) dataset

BNN-GAP8 shows good performance but the quantized network QNano-ACDNet clearly outperforms it for equivalent storage requirements. The computation requirements for BNN-GAP8 are given in MACs rather than FLOPs in [25]. Using the same re-scaling as detailed above, we arrive at 1768M FLOPs for BNN-GAP8. Our quantized network QNano-ACDNet compares very favorably, using only 19M FLOPs. In a nutshell, the pruned-and-quantized QNano-ACDNet delivers better performance than BNN-GAP8 XNOR with smaller resource requirements.

The performance of BNN-GAP8 on the 28-class problem is much better than the performance of the comparable XNOR network derived from ACDNet, XACDNet-GAP8. The results for the latter are consistent with the performance drop established for the slightly larger XMini-ACDNet on ESC30 (ESC50 reduced to 30 classes, cf. Table 5). How is it possible for BNN-GAP8 to achieve such good performance on a 30-class problem?

The likely reason is that BNN-GAP8 benefits from using spectrograms as input to the network. This means that in the BNN-GAP8 implementation much of the necessary full precision computation required is encapsulated outside of the network in the conversion of raw audio to spectrograms. The other XNOR networks in this comparison are deprived of this possibility since they perform end-to-end classification for raw audio input and thus must perform all required computation within the network.

From a pragmatic perspective, using spectrograms may be a useful approach for handling simple audio classification problems on MCUs that feature a DSP with hardware support for FFT computation, the basis of generating spectrograms. However, as has been shown in Table 7 and Figure 11, even where such support exists, forgoing it and using end-to-end classification with a pruned-and-quantized network instead still offers performance and resource benefits over the XNOR network. Furthermore, from the broader literature on DNN

audio classification, it is evident that purely spectrograms-based classification does not always allow us to reach state-of-the-art performance with conventional CNN architectures and that features learned from raw audio or multi-channel features are preferable for more difficult benchmarks [7], [8], [10], [11], [15].

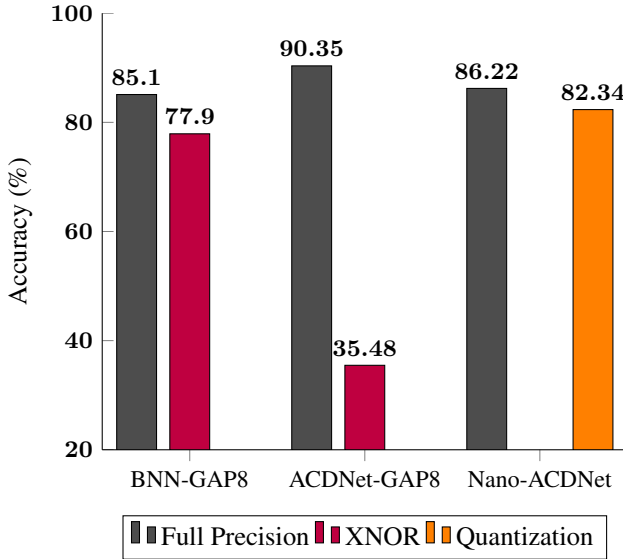


FIGURE 11. BNN-GAP8 [25], ACDNet-GAP8 and Nano-ACDNet accuracy on AudioEvent dataset for 28 classes. The full precision network for BNN-GAP8 is CNN-CNP [40].

Most of the work on XNOR nets so far has taken place in the image domain. A comparison to this work is instructive. We summarize the state-of-the-art for the most widely used datasets in Table 8. The accuracy achieved by XNOR nets is impressive (second last column) but it has to be noted that these nets are significantly larger than our target size. None of these models would fit on the relevant MCUs with the single exception of the one for MNIST. This is a very simple dataset with only 10 classes.

Datasets (#classes)	Full Precision		XNOR	
	Accuracy	Size (MB)	Accuracy	Size (MB)
MNIST (10)	99.87 [41]	5.8	99.23 [22]	0.10
CIFAR-10 (10)	99.50 [42]	2411	88.74 [23]	1.3
CIFAR-100 (100)	96.08 [43]	-	77.80 [24]	7.8
Imagenet (1000)	90.45 [44]	7030	71.20 [24]	7.8

TABLE 8. State-of-the-art accuracy (%) for various image datasets.

To verify whether our own results for audio classification are consistent with the image domain, we conducted additional experiments on image classification using XNOR. We have used an XNOR version of RESNET-18 [45] to classify the widely used benchmark image datasets CIFAR-10 and CIFAR-100. We created variably sized subsets of CIFAR-100 to see if the trend of the loss in accuracy is similar to audio classification. The experimental details are provided in Section IV. Table 9 and Figure 12 summarize the results. The sizes of the full precision models are between

42.63MB and 42.80MB and the computation requirements between 95.17M FLOPs and 95.21M FLOPs. For the XNOR-Net version, the model size is approximately 1.34MB using 2.06M FLOPs. The results of this experiment are consistent with those for the audio domain, and it is clearly visible that a similar performance drop for XNOR takes place as the number of classes increases.

Datasets	Full Precision	XNOR
	Accuracy (%)	Accuracy (%)
CIFAR-10	93.29	80.24
CIFAR-20	85.70	69.45
CIFAR-30	80.87	60.90
CIFAR-40	76.67	57.00
CIFAR-50	75.18	54.36
CIFAR-60	72.28	49.77
CIFAR-70	72.70	51.20
CIFAR-80	71.81	49.51
CIFAR-90	71.61	50.22
CIFAR-100	71.49	49.56

TABLE 9. RESNET-18 on CIFAR-10,20,30,....,100 datasets.

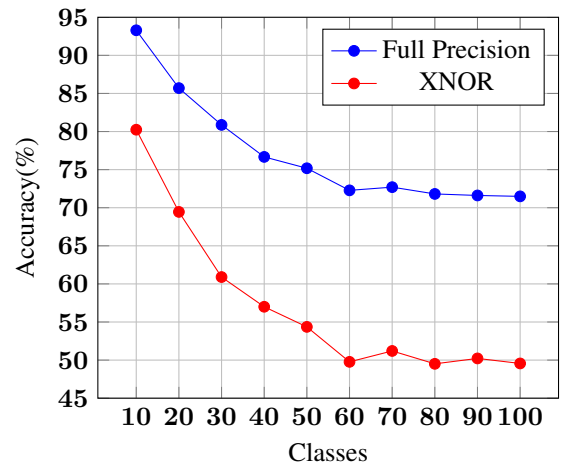


FIGURE 12. RESNET-18 on CIFAR-10,20,30,....,100 datasets

IV. EXPERIMENTAL DETAILS

All experiments were conducted with Python version 3.7.4 and GPU versions of Torch 1.8.1. All experimental codes are available at: <https://github.com/mohaimenz/pruning-vs-xnor>

A. DATASETS

The experiments are conducted on three widely used audio benchmark datasets - Environmental Sound (ESC-50 and ESC-10 [36]) and UrbanSound8k [37]. For the image classification experiments, we use the CIFAR-10 and CIFAR-100 benchmark image datasets.

ESC-50 contains 2000 samples that are equally distributed over 50 disjoint classes. The length of the audio samples are 5s recorded at 16kHz and 44.1kHz. Furthermore, the dataset is provided with a partitioning into 5 folds for cross

validation to help researchers achieve directly comparable results. ESC-10 is a subset of ESC-50 that has 400 audio samples distributed equally over 10 classes. The subsets of the ESC datasets are as follows:

S_{10} = The whole ESC-10 dataset
 $S_{20} = S_{10} \cup \{5, 31, 18, 27, 48, 8, 15, 45, 25, 34\}$
 $S_{30} = S_{20} \cup \{3, 14, 23, 36, 43, 7, 22, 28, 30, 49\}$
 $S_{40} = S_{30} \cup \{6, 9, 16, 17, 24, 29, 32, 35, 37, 44\}$
 S_{50} = The whole ESC-50 dataset

UrbanSound8k contains 8732 labeled audio samples of $\approx 4s$ each recorded at 22.05kHz. The data are pre-sorted into 10 folds and distributed over 10 classes for easy reproduction and comparison of performance of different algorithms.

AudioEvent dataset has 28 classes and 5223 samples unevenly distributed over the 28 classes. The data is recorded at 16kHz with bit depth of 16bit. The subsets of the AudioEvent datasets are as follows:

$S_{10} = \{0, 2, 5, 9, 11, 12, 17, 21, 25, 26\}$
 $S_{20} = S_{10} \cup \{1, 4, 7, 8, 14, 15, 19, 20, 23, 27\}$
 S_{28} = The whole AudioEvent dataset

The CIFAR-10 dataset has 60,000 image samples equally distributed over 10 classes. 50,000 of the samples are for training and 10,000 of them for testing. CIFAR-100 has 100 classes and 60,000 samples equally distributed across those classes. For each class, there are 500 training samples and 100 test samples. We create the subsets of CIFAR-100 using Equation 7. We define the subsets as follows:

$$S_{x_i} = S_{x_{i-1}} \cup \left\{ \frac{x}{10} + m \right\} \quad (9)$$

where $x \in \{10, 20, \dots, [n]\} \mid n \in [1, 100]$ and $m \in [1, 10]$. This would give us the following subsets such as:

S_{10} = The whole CIFAR-10 dataset.
 $s_{10} = \{0, 10, 20, 30, 40, 50, 60, 70, 80, 90\}$
 $S_{20} = s_{10} \cup \{1, 11, 21, 31, 41, 51, 61, 71, 81, 91\}$
 $S_{30} = S_{20} \cup \{1, 11, 21, 31, 41, 51, 61, 71, 81, 91\}$
 \dots
 \dots
 $S_{90} = S_{80} \cup \{9, 19, 29, 39, 49, 59, 69, 79, 89, 99\}$
 S_{100} = The whole CIFAR-100 dataset.

B. DATA PREPROCESSING

For the audio datasets (ESC-10, ..., 50 and UrbanSound8k), we train the DL models with samples of length 30,225, i.e., $\approx 1.51s$ audio at 20kHz (for AudioEvent dataset the length is 51,215, i.e., $\approx 3.2s$ audio at 16kHz). We use data augmentation as described in [14] and [9] for the audio datasets. For the image datasets we use random cropping, horizontal flipping, and rotation available in the Transforms module of the PyTorch TorchVision library.

All implementations of the data augmentation procedures are available in our GitHub repository.

C. MODELS AND HYPERPARAMETERS

The model configuration is available in the GitHub repository, and the hyperparameters for all the experiments conducted on the audio and image datasets are listed in Table 10.

V. SUMMARY

This paper presents the first study of XNOR-Net for end-to-end classification of raw audio. We emphasize state-of-the-art MCUs as practically important target architectures for realistic Edge-AI applications.

Whether or not XNOR is the technique of choice for such applications depends on the characteristics of the problem and data.

For small problem sizes, measured in the number of classes, our comprehensive experimental analysis shows that XNOR can produce models with good performance that are sufficiently small to fit the target architectures. This is the case where the associated full-precision network exceeds the memory capacity of the target architecture at most 32-fold. For larger models, it is necessary to use (pruning-based) model compression before XNOR is applied. For our test scenarios with small problem sizes, XNOR networks require significantly less computation than comparably sized models generated by pruning-and-quantization alone. For relatively simple problems, the performance of XNOR on MCUs can be further increased by using spectrograms as input to the net. This enable us to capitalize on special DSP hardware so that the full-precision computations required to handle raw audio can be confined outside of the net in the spectrogram generation. All of this makes XNOR well-suited for MCU targets and problems with few classes.

The picture changes as the problem complexity grows and larger numbers of classes need to be distinguished. Our analysis shows that XNOR-Nets face large drops in classification accuracy for datasets with many classes. This performance degradation is much more rapid than that of their pruning-and-quantization counterparts. Comparably sized models generated by pruning-and-quantization show significantly better performance while still satisfying the constraints of the target architectures. The advantages of spectrogram-based network input can no longer be exploited with complex data characteristics as feature-learning from raw audio or multi-channel input are required to reach state-of-the-art performance.

This renders pruning-and-quantization the preferred approach from a certain problem complexity unless computation speed rather than model size dominates the decision.

Furthermore, to the best of our knowledge, there is no off-the-shelf computation kernel for XNOR-Nets yet. This means that it is difficult to realize the theoretical advantage on existing add-multiplication based hardware and that custom hardware is required to achieve the full benefit of faster computation [46]. However, given the popularity of XNOR nets we are hopeful that such support is not too far away.

Datasets→ Models→ Hyperparams↓	ESC10,....,50			UrbanSound8k			CIFAR-10,....,100	
	ACDNet	Micro-ACDNet	XMicro-ACDnet	ACDnet	Micro-ACDNet	XMicro-ACDNet	RESNET-18	XNOR-RESNET-18
Input shape (ch, h, w)	(1, 1, 30225)						(3, 32, 32)	
Loss function	KLD			KLD			CE	
Optimizer	SGD		ADAM	SGD		ADAM	SGD	ADAM
Weight decay	5e-4		1e-4	5e-4		1e-4	5e-4	1e-4
Momentum	0.9		-	0.9		-	0.9	-
Initial LR	0.1		0.001	0.1		0.001	0.1	0.001
Epochs	2000			1200			400	
LR Scheduler	(600,1200,1800)		CosAnLR	(600,1200,1800)		CosAnLR	CosAnLR	
Warmup epochs	10		-	10		-	-	
LR decay	0.1x		-	0.1x		-	-	
Batch size	64							

TABLE 10. Hyperparameter settings for experiments conducted on ESC10, ..., 50, UrbanSound8k, and CIFAR-10, ..., 100 datasets. In this table, the loss functions KLD stands for KL Divergence, CE for Cross Entropy. SGD stands for Stochastic Gradient Descent and ADAM for Adaptive Momentum Estimation. In the LR Scheduler row, CosAnLR stands for CosineAnnealingLR.

REFERENCES

- [1] Matthias Auf der Mauer, Tristan Behrens, Mahdi Derakhshanmanesh, Christopher Hansen, and Stefan Muderack. Applying sound-based analysis at porsche production: Towards predictive maintenance of production machines using deep learning and internet-of-things technology. In *Digitalization Cases*, pages 79–97. Springer, 2019.
- [2] Feng Jia, Yaguo Lei, Liang Guo, Jing Lin, and Saibo Xing. A neural network constructed by deep learning technique and its application to intelligent fault diagnosis of machines. *Neurocomputing*, 272:619–628, 2018.
- [3] Huitaek Yun, Hanjun Kim, Eunseob Kim, and Martin BG Jun. Development of internal sound sensor using stethoscope and its applications for machine monitoring. *Procedia Manufacturing*, 48:1072–1078, 2020.
- [4] Roneel V Sharan and Tom J Moir. An overview of applications and advancements in automatic sound recognition. *Neurocomputing*, 200:22–34, 2016.
- [5] Dan Stowell, Tereza Petrusková, Martin Šálek, and Pavel Linhart. Automatic acoustic identification of individuals in multiple species: improving identification across recording conditions. *Journal of the Royal Society Interface*, 16(153):20180940, 2019.
- [6] Xiao Yan, Hemin Zhang, Desheng Li, Daifu Wu, Shiqiang Zhou, Mengmeng Sun, Haiping Hu, Xiaoqiang Liu, Shijie Mou, Shengshan He, et al. Acoustic recordings provide detailed information regarding the behavior of cryptic wildlife to support conservation translocations. *Scientific reports*, 9(1):1–11, 2019.
- [7] Yuan Gong, Yu-An Chung, and James Glass. Ast: Audio spectrogram transformer. arXiv preprint arXiv:2104.01778, 2021.
- [8] Loris Nanni, Gianluca Maguolo, Sheryl Brahmam, and Michelangelo Paci. An ensemble of convolutional neural networks for audio classification. *Applied Sciences*, 11(13):5796, 2021.
- [9] Md Mohaimenuzzaman, Christoph Bergmeir, Ian Thomas West, and Bernd Meyer. Environmental sound classification on the edge: Deep acoustic networks for extremely resource-constrained devices. arXiv e-prints, pages arXiv–2103, 2021.
- [10] Jaehun Kim. Urban sound tagging using multi-channel audio feature with convolutional neural networks. *Proceedings of the Detection and Classification of Acoustic Scenes and Events*, 2020.
- [11] Anurag Kumar and Vamsi Ithapu. A sequential self teaching approach for improving generalization in sound event recognition. In *International Conference on Machine Learning*, pages 5447–5457. PMLR, 2020.
- [12] Zhichao Zhang, Shugong Xu, Shunqing Zhang, Tianhao Qiao, and Shan Cao. Learning attentive representations for environmental sound classification. *IEEE Access*, 7:130327–130339, 2019.
- [13] Yu Su, Ke Zhang, Jingyu Wang, and Kurosh Madani. Environment sound classification using a two-stream cnn based on decision-level fusion. *Sensors*, 19(7):1733, 2019.
- [14] Yuji Tokozume, Yoshitaka Ushiku, and Tatsuya Harada. Learning from between-class examples for deep sound recognition. In *International Conference on Learning Representations (ICLR)*, page Not available, 2018.
- [15] Hardik B Sailor, Dharmesh M Agrawal, and Hemant A Patil. Unsupervised filterbank learning using convolutional restricted boltzmann machine for environmental sound classification. In *INTERSPEECH*, pages 3107–3111, 2017.
- [16] Song Han, Huizi Mao, and William J. Dally. Deep compression: Compressing deep neural network with pruning, trained quantization and Huffman coding. In *4th International Conference on Learning Representations (ICLR)*, page Not available, 2016.
- [17] Xiaolong Ma, Geng Yuan, Sheng Lin, Zhengang Li, Hao Sun, and Yanzhi Wang. Resnet can be pruned 60×: Introducing network purification and unused path removal (p-rm) after weight pruning. In *2019 IEEE/ACM International Symposium on Nanoscale Architectures (NANOARCH)*, pages 1–2. IEEE, 2019.
- [18] Pavlo Molchanov, Stephen Tyree, Tero Karras, Timo Aila, and Jan Kautz. Pruning convolutional neural networks for resource efficient inference. In *5th International Conference on Learning Representations (ICLR)*, page Not available, 2017.
- [19] Oyebade Oyedotun, Djamila Aouada, and Bjorn Ottersten. Structured compression of deep neural networks with debiased elastic group lasso. In *The IEEE Winter Conference on Applications of Computer Vision*, pages 2277–2286, 2020.
- [20] Geoffrey Hinton, Oriol Vinyals, and Jeff Dean. Distilling the knowledge in a neural network. *stat*, 1050:9, 2015.
- [21] Antonio Polino, Razvan Pascanu, and Dan Alistarh. Model compression via distillation and quantization. In *International Conference on Learning Representations (ICLR)*, page Not available, 2018.
- [22] Mohammad Rastegari, Vicente Ordonez, Joseph Redmon, and Ali Farhadi. Xnor-net: Imagenet classification using binary convolutional neural networks. In *European conference on computer vision*, pages 525–542. Springer, 2016.
- [23] Cong Wang. coo0o0rn/pytorch-xnor-net: Xnor-net, with binary gemm and binary conv2d kernels, support both cpu and gpu. <https://github.com/coo0o0rn/pytorch-xnor-net>.
- [24] Adrian Bulat, Brais Martinez, and Georgios Tzimiropoulos. High-capacity expert binary networks. In *International Conference on Learning Representations*, 2020.
- [25] Gianmarco Cerutti, Renzo Andri, Lukas Cavigelli, Elisabetta Farella, Michele Magno, and Luca Benini. Sound event detection with binary neural networks on tightly power-constrained iot devices. In *Proceedings of the ACM/IEEE International Symposium on Low Power Electronics and Design*, pages 19–24, 2020.
- [26] Daniel Rothmann. What’s wrong with spectrograms and cnns for audio processing? <https://towardsdatascience.com/whats-wrong-with-spectrograms-and-cnns-for-audio-processing-311377d7ccd>, Mar 2018.
- [27] L Wyse. Audio spectrogram representations for processing with convolutional neural networks. In *Proceedings of the First International Conference on Deep Learning and Music*, Anchorage, US, May, 2017., pp. 37–41, pages 37–41, 2017.
- [28] Kartik Chaudhary. Understanding audio data, fourier transform, fft, spectrogram and speech recognition. <https://towardsdatascience.com/understanding-audio-data-fourier-transform-fft-spectrogram-and-speech-recognition-a4072d228520>, Jun 2021.
- [29] Prateek Verma and Julius O Smith. Neural style transfer for audio spectrograms. arXiv preprint arXiv:1801.01589, 2018.

- [30] Sajid Anwar, Kyuyeon Hwang, and Wonyong Sung. Structured pruning of deep convolutional neural networks. *ACM Journal on Emerging Technologies in Computing Systems (JETC)*, 13(3):32, 2017.
- [31] Ariel Gordon, Elad Eban, Ofir Nachum, Bo Chen, Hao Wu, Tien-Ju Yang, and Edward Choi. Morphnet: Fast & simple resource-constrained structure learning of deep networks. In *Proceedings of the IEEE Conference on Computer Vision and Pattern Recognition (CVPR)*, pages 1586–1595, 2018.
- [32] Hao Li, Asim Kadav, Igor Durdanovic, Hanan Samet, and Hans Peter Graf. Pruning filters for efficient convnets. In *5th International Conference on Learning Representations (ICLR)*, page Not available, 2017.
- [33] Jian-Hao Luo, Hao Zhang, Hong-Yu Zhou, Chen-Wei Xie, Jianxin Wu, and Weiyao Lin. Thinet: pruning cnn filters for a thinner net. *IEEE transactions on pattern analysis and machine intelligence*, 2018.
- [34] Pravendra Singh, Vinay Kumar Verma, Piyush Rai, and Vinay Namboodiri. Leveraging filter correlations for deep model compression. In *The IEEE Winter Conference on Applications of Computer Vision*, pages 835–844, 2020.
- [35] Jian-Hao Luo and Jianxin Wu. Autopruner: An end-to-end trainable filter pruning method for efficient deep model inference. *Pattern Recognition*, 107:107461, 2020.
- [36] Karol J. Piczak. ESC: Dataset for Environmental Sound Classification. In *Proceedings of the 23rd Annual ACM Conference on Multimedia*, pages 1015–1018. ACM Press, 2015.
- [37] Justin Salamon, Christopher Jacoby, and Juan Pablo Bello. A dataset and taxonomy for urban sound research. In *Proceedings of the 22nd ACM international conference on Multimedia*, pages 1041–1044. ACM, 2014.
- [38] Zechun Liu, Baoyuan Wu, Wenhan Luo, Xin Yang, Wei Liu, and Kwang-Ting Cheng. Bi-real net: Enhancing the performance of 1-bit cnns with improved representational capability and advanced training algorithm. In *Proceedings of the European conference on computer vision (ECCV)*, pages 722–737, 2018.
- [39] Naoya Takahashi, Michael Gygli, Beat Pfister, and Luc Van Gool. Deep convolutional neural networks and data augmentation for acoustic event detection. *arXiv preprint arXiv:1604.07160*, 2016.
- [40] Matthias Meyer, Lukas Cavigelli, and Lothar Thiele. Efficient convolutional neural network for audio event detection. *arXiv preprint arXiv:1709.09888*, 2017.
- [41] Adam Byerly, Tatiana Kalganova, and Ian Dear. No routing needed between capsules. *arXiv preprint arXiv:2001.09136v6*, 2021.
- [42] Alexey Dosovitskiy, Lucas Beyer, Alexander Kolesnikov, Dirk Weissenborn, Xiaohua Zhai, Thomas Unterthiner, Mostafa Dehghani, Matthias Minderer, Georg Heigold, Sylvain Gelly, et al. An image is worth 16x16 words: Transformers for image recognition at scale. *arXiv preprint arXiv:2010.11929*, 2020.
- [43] Mingxing Tan and Quoc Le. Efficientnet: Rethinking model scaling for convolutional neural networks. In *International Conference on Machine Learning*, pages 6105–6114. PMLR, 2019.
- [44] Xiaohua Zhai, Alexander Kolesnikov, Neil Houlsby, and Lucas Beyer. Scaling vision transformers. *arXiv preprint arXiv:2106.04560*, 2021.
- [45] Kaiming He, Xiangyu Zhang, Shaoqing Ren, and Jian Sun. Deep residual learning for image recognition. In *Proceedings of the IEEE conference on computer vision and pattern recognition (CVPR)*, pages 770–778, 2016.
- [46] Benoit Jacob, Skirmantas Kligys, Bo Chen, Menglong Zhu, Matthew Tang, Andrew Howard, Hartwig Adam, and Dmitry Kalenichenko. Quantization and training of neural networks for efficient integer-arithmetic-only inference. In *Proceedings of the IEEE conference on computer vision and pattern recognition*, pages 2704–2713, 2018.



MD MOHAIMENUZZAMAN is currently pursuing the PhD degree in data science from the Department of Data Science and AI, Faculty of Information Technology at Monash University, Australia. He received his B.Sc and M.Sc in computer science and engineering in 2007 and 2013 respectively.

Before commencing in PhD, he developed software applications for international clients for about a decade. Currently, he also works as a teaching associate for the faculty of information technology where he teaches data science and software engineering related courses. He received the "2020 Faculty Teaching Excellence" award for teaching "Introduction to Data Science" to graduate students.



CHRISTOPH BERGMEIR is a Senior Lecturer in Data Science and Artificial Intelligence at Monash University. He holds a PhD in Computer Science from the University of Granada, Spain, and an M.Sc. degree in Computer Science from the University of Ulm, Germany.

He is a 2019 ARC DECRA Fellow in the Department of Data Science and AI at Monash University where he develops "efficient and effective analytics for real-world time series forecasting".

He works as a Data Scientist in a variety of projects with external partners in diverse sectors, e.g. in healthcare or infrastructure maintenance. He has published on time series prediction using Machine Learning methods, recurrent neural networks and long short-term memory neural networks (LSTM), time series predictor evaluation, as well as on medical applications and software packages in the R programming language, in journals such as *IEEE Transactions on Neural Networks and Learning Systems*, *Journal of Statistical Software*, *Computational Statistics and Data Analysis*, and *Information Sciences*.



BERND MEYER is a Professor in the Department of Data Science and AI, Faculty of Information Technology at Monash University, Australia. He received his PhD in computer science in 1994 from University of Hagen, Germany.

He works on data-intensive computational ecology, develops mathematical and computational models for the interactions of organisms with their environment, mostly focusing on the collective behaviour of social insects, such as bees and ants.

How these self-organised "super-organisms" coordinate their actions remains a fascinating enigma. also works on AI-based methods for monitoring animal activity as the basis for ecosystem monitoring and for automating experiments.

...